Nano-Structures & Nano-Objects 46 (2026) 101672

Contents lists available at ScienceDirect

Nano-Structures & Nano-Objects

journal homepage: www.elsevier.com/locate/nanoso

Graphene nanofluids for sustainable automotive cooling: Mitigating contamination effects and enhancing engine radiator performance

Clint K S [a], Stephen Raj Jhonson [a], Kumaran Kadirgama [a,b,c,*], Lingenthiran Samylingam [d], Navid Aslfattahi [e], Maryam Sadat Kiai [f,g], Chee Kuang Kok [d,**], Wan Sharuzi Wan Harun [a,c,h], A.S. Veerendra [i], Sivaraos Subramonian [j,**]

[a] Faculty of Mechanical Automotive Engineering Technology, Universiti Malaysia Pahang Al-Sultan Abdullah, Pekan, Pahang, Malaysia
[b] Centre for Research in Advanced Fluid Processes, Universiti Malaysia Pahang Al-Sultan Abdullah, Gambang, Pahang 26300, Malaysia
[c] Centre for Sustainable Materials and Surface Metamorphosis (CSMSM), Chennai Institute of Technology, Chennai, India
[d] Center for Advanced Mechanical and Green Technology, Center of Excellence for Robotics & Sensing Technologies, Faculty of Engineering and Technology, Multimedia University, Jalan Ayer Keroh Lama, Bukit Beruang, Melaka 75450, Malaysia
[e] Department of Fluid Dynamics and Thermodynamics, Faculty of Mechanical Engineering, Czech Technical University in Prague, Technická 4, Prague 160 00, Czech Republic
[f] Center for BioNano Interactions, School of Chemistry, University College of Dublin, Belfield, Dublin 4, Ireland
[g] Nano-Science and Nano-Engineering Program, Graduate School of Science, Engineering and Technology Istanbul Technical University Istanbul, 34469, Turkey
[h] Automotive Engineering Centre, Universiti Malaysia Pahang Al-Sultan Abdullah, Pekan, Pahang 26600, Malaysia
[i] Department of Electrical and Electronics Engineering, Manipal Institute of Technology, Manipal Academy of Higher Education, Manipal, Karnataka 576104, India
[j] Centre of Smart System and Innovative Design, Faculty of Industrial and Manufacturing Engineering and Technology, Universiti Teknikal Malaysia Melaka, Durian Tunggal, Melaka 76100, Malaysia

ARTICLE INFO

Keywords:
Graphene nanofluids
Thermal conductivity
Heat transfer enhancement
Nanofluid characterization
Engine cooling

ABSTRACT

Resourceful thermal management systems are critical for modern automotive engines, particularly as the industry moves toward high-performance, fuel-efficient vehicles, where conventional engine coolants suffer from inherently low thermal conductivity, limiting heat dissipation efficiency. With approximately 33% of combustion energy wasted as heat and traditional cooling enhancement methods reaching their operational limits, there is an urgent need for innovative coolant technologies to meet the demands of compact engine designs and higher power densities. While extensive research exists on metal oxide nanofluids for automotive applications, investigations into graphene-based nanofluids for car radiators remain limited, with most studies focusing solely on thermophysical property enhancement without considering real-world contamination effects, creating a significant knowledge gap regarding practical implementation and long-term performance reliability. This research aimed to synthesize graphene nanofluids with PLLR coolant, evaluate their thermal conductivity and viscosity properties, determine heat dissipation performance in car radiators, and investigate the impact of contamination on cooling efficiency. In this research GNP@PLLRC nanofluids were prepared at concentrations of 0.01%, 0.03%, 0.05%, 0.07%, and 0.09% (wt%) using a two-step method involving magnetic stirring and sonication, with comprehensive characterization performed using FTIR, XRD, SEM-EDX, and UV-Vis spectroscopy, while thermal conductivity and viscosity were measured using the METER Tempos Analyzer and Brookfield Viscometer, respectively, and performance evaluation was conducted using a Perodua Kancil cooling system with cyclic tests of 30 min and 1 h duration. Results showed a strong synergistic effect between temperature (30–70°C) and graphene concentration, with 0.09 wt% achieving optimal thermal conductivity (0.443 W/m·K at 70°C) and lowest viscosity (2.34 cP at 70°C), outperforming the base fluid. Contamination reduced thermal conductivity by up to 30% and cooling efficiency by 8%, confirming the critical importance of system cleanliness for reliable automotive cooling performance. This research investigates and attempts to close the gap by using and experimentally measuring the effects of GNP-PLLRC NF in full automotive radiators. This research systematically measuring the effect of realistic coolant contamination on the heat dissipating. This study represents a novel radiator-scale investigation that combines graphene-based coolants considering contamination and illustrates

* Corresponding author at: Faculty of Mechanical Automotive Engineering Technology, Universiti Malaysia Pahang Al-Sultan Abdullah, Pekan, Pahang, Malaysia.
** Corresponding authors.
E-mail addresses: kumaran@umpsa.edu.my (K. Kadirgama), ckkok@mmu.edu.my (C.K. Kok), sivarao@utem.edu.my (S. Subramonian).

https://doi.org/10.1016/j.nanoso.2026.101672
Received 21 October 2025; Received in revised form 2 January 2026; Accepted 28 April 2026
Available online 5 May 2026

their potential application in high-performance compact engines. This research validates graphene nanofluids as superior alternatives to conventional coolants, offering potential for compact radiator designs with enhanced cooling efficiency, with significant implications for high-performance and electric vehicle applications, while highlighting the critical need for contamination-resistant formulations in practical automotive thermal management systems.

1. Introduction

The automotive industry's need for more efficient thermal management systems grows as modern engines run at higher power densities and temperatures [1,2]. Engine coolants are essential for vehicle thermal management, absorbing excess heat from combustion and transferring it to the radiator for release into the environment, thus maintaining optimal operating temperatures [3]. Traditional automotive coolants are mainly made of deionized water, ethylene glycol, and additives for corrosion, foam, and pH control stabilizing chemicals [4, 5]. While traditional coolants have met industry needs for decades, their thermal limitations are now more evident as engines become more powerful and compact [6]. Nanotechnology has opened new opportunities to improve heat transfer fluids by creating 'nanofluid-engineered' colloidal suspensions of nanoparticles dispersed in traditional base fluids [7,8]. Since their introduction by researchers at leading national laboratories worldwide, nanofluids have shown remarkable potential to enhance thermophysical properties, including thermal conductivity, convective heat transfer coefficients, and thermal diffusivity [9,10]. These improvements arise from the unique properties of nanoparticles, which possess thermal conductivities much greater than those of base fluids, allowing for substantial performance gains even at low concentrations 1% [11]. Of all nanoparticles considered for nanofluids, graphene stands out for its outstanding thermal properties [12]. Graphene has a very high theoretical thermal conductivity of about 5000 W/mK [13]. This is much higher than conventional nanoparticles such as aluminum oxide (25–40 W/mK) [14] and copper oxide (78 W/mK) [15]. Graphene also outperforms other carbon-based materials. Graphene's two-dimensional honeycomb structure offers excellent thermal transport [16], making it an ideal choice for improving the thermal performance of automotive coolants. Despite the promising thermal properties of graphene, research specifically focused on graphene-based nanofluids in automotive radiator applications remains relatively limited compared to studies on other nanoparticle types [17]. Fig. 1 shows various studies conducted in the recent past in this domain. The automotive industry is moving toward lighter, more compact vehicle. There is a growing demand for fuel-efficient vehicles. This has created an urgent need for advanced cooling solutions that can effectively manage the increased heat loads. These solutions must avoid larger cooling system components that would add weight and reduce fuel economy [18]. The automotive thermal management systems faces fundemtnal challenges. Conventional heat transfer solutions have inherently reduced thermal conductivity of, which represents the primary obstacle to developing high-performance cooling systems [19]. Current automotive engines waste approximately 33% of the energy generated from combustion as heat. If this excess thermal energy is not adequately dissipated, it leads to engine overheating. It can also lead to lubricating oil degradation, weakening of engine component materials, and accelerated wear between moving parts [20,21]. Traditional methods for enhancing radiator cooling performance, such as increasing fin density and implementing microchannels, have reached their practical limits in terms of effectiveness and cost-efficiency [22]. Modern automotive design has conflicting requirements. Vehicle need to be lighter, more compact, and more efficient. At the same time they required enhanced cooling performance. These demands cannot be adequately addressed through conventional cooling system modifications [23–25]. The need for increased pumping power to circulate conventional coolants through larger cooling systems further reduces overall engine efficiency and fuel economy, creating a counterproductive cycle [26]. Some studies show dispersing graphene or graphene-oxide nanoparticles in standard $H_2O/C_2H_6O_2$ in coolants enhances the convective heat transfer coefficient by up to 111%@0.006 vol%,170%@0.5 vol%, 85%@0.1 vol% for DPHE, allowing for a smaller, lighter radiator while preserving engine cooling performance [27–29]. In some analyses of radiator tests using GNP@CNC fluids, the convective heat transfer coefficient increased by 51.91%, the overall heat transfer coefficient by up to 46.72%, and the

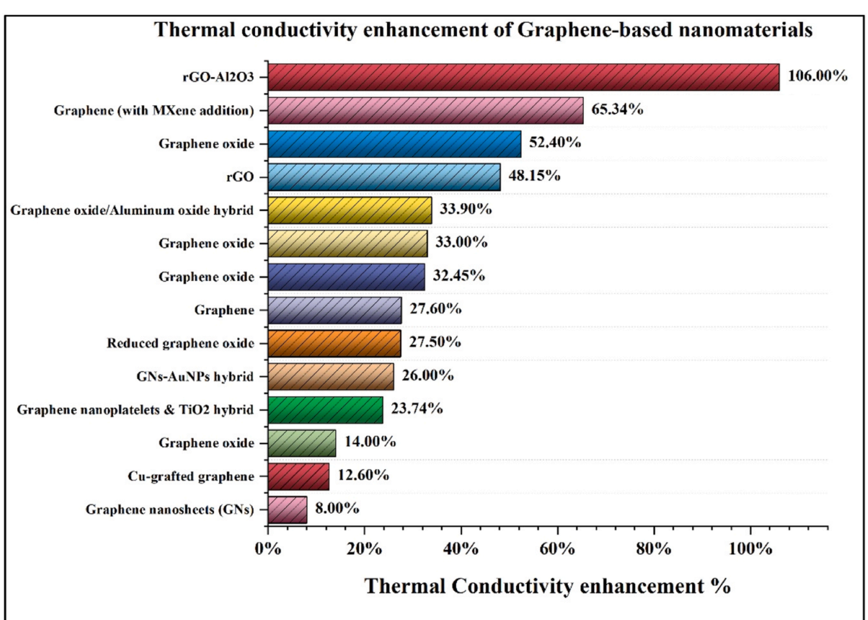

Fig. 1. Thermal conductivity enhancement of Graphene-based nanomaterials. (data summarized from supplementary Table S1).

cooling effectiveness by up to 92.4% compared to conventional coolants [30].

In other similar analyses, the CHTC is found to be 30.93% on graphene@water and 53.83% on graphene@CNC, respectively [31,32]. Optimizing concentration is key factor, 0.001–0.01% yields big temperature drops (up to 17.9x) with minimal viscosity increase, 0.01–0.05% maximizes thermal conductivity, and > 0.1% shows diminishing returns [32–34]. Stability tests show graphene oxide nanofluids maintain uniform dispersion through 50 freeze-thaw cycles and extended high-temperature exposure, with surface treatments and hybrid formulations enhancing long-term stability [35–38]. Low-concentration graphene nanofluids enable 20–30% radiator downsizing without losing cooling performance, improve fuel efficiency, and help engine parts last longer by reducing thermal stress [30, 34]. Fig. 2 shows the comparative studies of Graphene with metal oxide nanofluids. Recent research includes covalently functionalized graphene nanoplatelets for better turbulent heat transfer, surface-modified graphene for stability. Ethylene glycol water graphene mixtures for extreme cooling, with industrial trials showing 0.380 W/mK at 85 °C with 0.1 wt % [35,39,40]. Together, these advances make graphene-based nanofluids a promising choice for next-generation automotive cooling, enabling smaller, more efficient systems with major economic and environmental benefits.

This study seeks to tackle significant thermal regulation issues. It methodically examines graphene-infused nanofluids as next-generation automotive coolants. Stable graphene nanofluids are prepared using commercial coolant as the base liquid. Concentrations are varied between 0.01% and 0.09% by weight. It also thoroughly analyzes the thermophysical attributes of these nanofluids. Special attention has been given to thermal conductivity and viscosity across a range of temperatures, along with assessing the heat dissipation capacity of graphene nanofluids. This is done within actual automotive radiator systems, using the Perodua Kancil's cooling mechanism as the test framework. Furthermore, this research addresses a crucial deficiency in existing nanofluid studies. It examines how real-world impurities such as oil, corrosion, debris, and scaling impact the effectiveness of graphene-based nanofluids. These elements frequently neglected in laboratory research but vital for real-world automotive use. Through repeated testing at intervals of 30 min and 1 h, this aims to deliver meaningful findings regarding the durability and operational behavior of graphene nanofluids under conditions that closely reflect genuine automotive environments. The findings from this investigation are expected to contribute knowingly to the advancement of next-generation automotive cooling technologies. They may enable more efficient thermal management in high-performance and electric vehicles. These results also support the industry's ongoing efforts toward improved fuel efficiency and reduced environmental impact.

2. Materials and methods

2.1. Graphene nanoparticles (GNPs)

Graphene nanoparticles (GNPs) are 2D, sp^2-hybridised carbon sheets with outstanding thermal conductivity (over 2000 W/mK) and high aspect ratios, enabling efficient heat transfer in nanofluids [41,42]. Their flat, ultra-thin structure provides a high surface-to-volume ratio, enhancing Brownian motion and micro convection in fluids [43,44]. Functionalization methods like PEG grafting or surfactant-free dispersion ensure stable, uniform suspensions in ethylene glycol@water mixtures at 0.01–0.1% volume fractions [36,41]. Graphene nanoplatelets are lightweight, chemically inert, and compatible with standard antifreeze, allowing easy integration without affecting pH or inhibitors [45]. Studies already conducted combining graphene nanoplatelets with cellulose nanocrystals increased the convective heat-transfer coefficient by 51.9% and the overall heat-transfer coefficient by 46.7% versus a water-EG baseline [46,47]. Pressure drops increased moderately, making it a favorable trade-off for forced convection systems. Also, some CFD simulations conducted state that adding 0.09 vol% graphene oxide to 60:40 water–EG blends, along with louvered tubes, boosts heat-transfer coefficients by over 236%, confirming graphene's

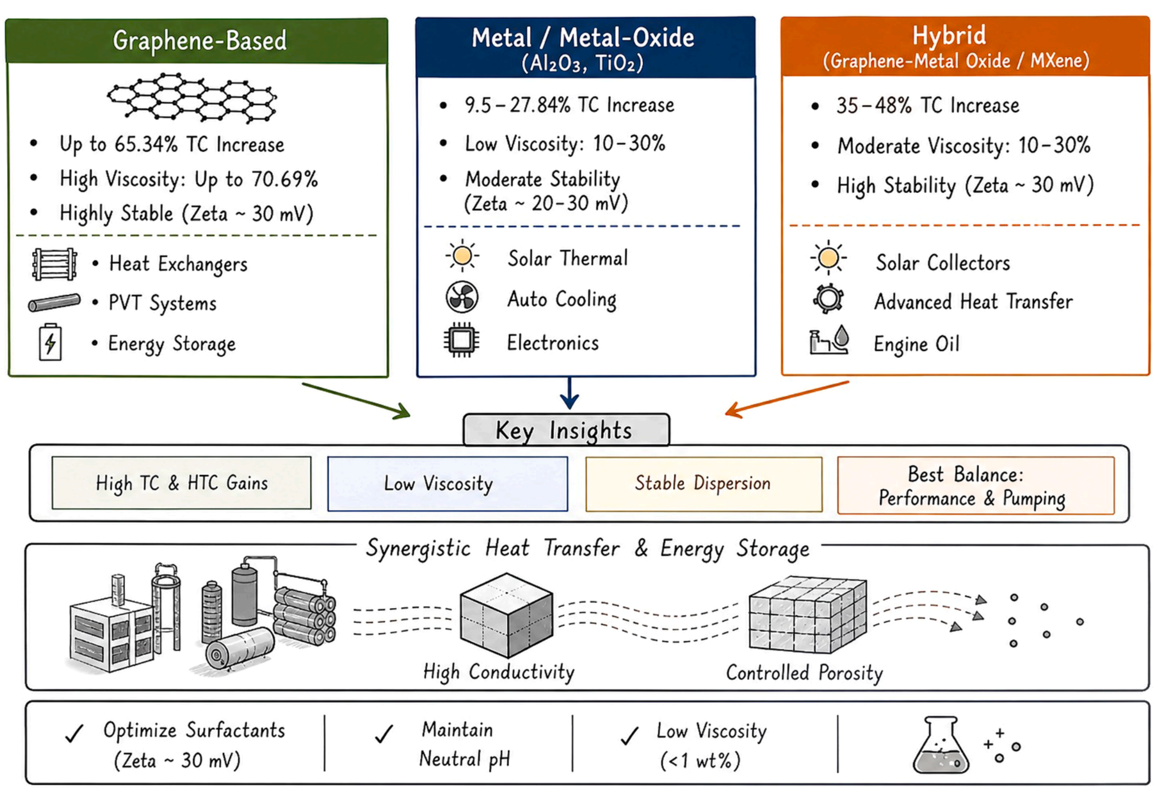

Fig. 2. Comparative Performance: Graphene vs. Metal/Metal- Oxide Nanofluids.

effectiveness with advanced radiator designs [32]. Adding GNPs increases thermal conductivity by 20–60% and induces shear-thinning, non-Newtonian behavior at higher concentrations, lowering pumping power in turbulent flow [36]. Optimal GNP concentrations (0.05–0.1 vol%) maximize conductivity while minimizing viscosity and agglomeration, ensuring long-term stability. Advanced functionalization and ultrasonication provide dispersions that remain stable for weeks, sustaining radiator performance. Thus, graphene nanoparticles are a game changing additive for high performance radiator fluids.

2.2. Characterization of nanoparticles

Nanoparticle characterization is essential in studying how contaminants affect coolant efficiency and engine performance, as it confirms the material's structure and integrity. Using SEM, XRD, and FTIR together offers a thorough analysis of graphene's properties. SEM analysis using the JEOL JSM-IT200 (up to 30,000X magnification, 1–30 kV, SE/BSE detector) shows the surface features and particle size of graphene nanoparticles. It confirms thin, sheet-like structures, indicates agglomeration, and reveals surface textures and defects, which are vital for understanding graphene's stability and its effect on coolant and engine performance. XRD analysis with a PANalytical X'Pert^3 Powder diffractometer provides detailed structural data on graphene nanoparticles, identifying crystallinity, interlayer spacing, and purity. A sharp peak at $2\theta = 26^{\circ}$ confirms the graphitic layered structure [48], while the absence of extra peaks shows high purity. These factors are directly linked to the nanoparticles' conductivity and their impact on coolant performance. FTIR analysis using the Thermo Fisher Nicolet iS50 (600–4000 cm^{-1}) identifies chemical bonds and surface groups on graphene. Key absorption bands reveal graphitic structures and any surface oxidation or modifications, helping to detect contaminants that may affect how graphene interacts with coolant and influence engine performance. Together, SEM, XRD, and FTIR accurately identify and validate graphene nanoparticles, set baseline properties for assessing contamination effects, and offer key structural and compositional insights needed to interpret changes in coolant efficiency and engine performance.

2.3. Radiator Coolant

PETRONAS Long-Life Radiator Coolant (PLLRC) uses an ethylene glycol base for year-round protection taken as base fluid. It has a gravity of 1.136 g/cm^3 at 20°C, freeze protection down to −36.4°C (50% dilution), and a high boiling point of 167°C undiluted. Its mildly alkaline pH (7.4–7.5) and strong buffering (8.6 mL) prevent corrosion, ensuring up to 20,000 km or one year of effective service. Table 1 provided a detailed thermophysical properties of PLLRC. Petronas coolant's corrosion inhibitors protect all major metals year-round and are compatible with seals and hoses, preventing swelling and degradation. Its silicone, amine, borate, and silicate-free formula avoids deposits and scale, ensuring radiator efficiency. Non-foaming and cavitation protection additives maintain stable heat transfer and protect water pumps, while the formula resists viscosity and performance changes even at extreme temperatures. The coolant is mixed 1:2 with water for best performance and is green for easy identification and leak detection.

Table 1
Thermophysical properties of PLLRC coolant.

Characteristics	Typical value
Gravity 20°C (g/cm^3)	1.136
Freezing point, °C (50% diluted with distilled water)	-36.4
Freezing point, °C (30% diluted with distilled water)	-15.6
Boiling Point, °C (undiluted)	167
pH Value (undiluted)	8.1
pH Value (50% water)	7.5
pH Value (70% water)	7.4
Reserved Alkalinity	8.6
Colour	Greenish
Water Content, max % vol	3.5

2.4. Preparation of nano fluids

Graphene nanoparticle (GNP)–based nanofluids were prepared using PETRONAS Long-Life Radiator Coolant (PLLRC; high-temperature resistant, green) as the base fluid due to its durability and suitability for high-temperature applications. Five nanofluid samples were prepared with different GNP concentrations, each with a total volume of 200 mL. Each sample was stirred with a sterilized magnetic stir bar on a magnetic stirrer at moderate speed (500 rpm) for 30 min to initiate homogenization and break up loosely bound agglomerates [49]. Following probe sonication, the samples were transferred to an ultrasonic bath and sonicated for an additional 30 min. Bath temperature was monitored and maintained below the coolant's thermal tolerance to prevent property degradation. After sonication, each nanofluid sample was transferred into a sealed, inert container and stored under controlled environmental conditions for 14 days to assess sedimentation stability. No visible sediment was observed, and the sample showed a uniform appearance, indicating satisfactory colloidal stability. Fig. 3. showing the synthesis steps of GNP@PLLRC. All preparation steps were performed promptly and consistently to ensure repeatability of results.

2.5. Measurement of thermal conductivity

The thermal conductivity of GNP@PLLRC nanofluids at concentrations of 0.01, 0.03, 0.05, 0.07, and 0.09 wt% was measured using a METER TEMPOS thermal analyzer equipped with a KS-3 thermal conductivity sensor. Before measurement, each nanofluid sample was thoroughly mixed to ensure homogeneous dispersion of nanoparticles. The prepared sample was then poured into a clean container, taking care to eliminate any entrapped air bubbles that could affect thermal measurements. The thermal analyzer was powered on and allowed to complete internal self-check procedures. The KS-3 sensor was calibrated according to the manufacturer's guidelines before use. During measurement, the sensor probe was fully inserted into the sample, ensuring no contact with the container's walls or base to avoid heat conduction interference. The temperature of each sample was maintained constant throughout testing to minimize temperature-dependent variations in thermal conductivity. For each concentration, the measurement was initiated, and the thermal conductivity reading was recorded once the value stabilized. Between measurements, the KS-3 sensor was thoroughly cleaned and dried to prevent cross-contamination between samples. All measurements were conducted under identical environmental conditions to ensure repeatability and accuracy. Fig. 4 shows the functional parts of the thermal analyzer in practical applications.

2.6. Measurement of dynamic viscosity

The dynamic viscosity of GNP@PLLRC nanofluids at various weight fractions (0.01, 0.03, 0.05, 0.07, and 0.09 wt%) was measured over the temperature range of 30–70 °C using a Brookfield DV-III Ultra programmable rheometer equipped with a TC-550 temperature-controlled water bath. The water bath was filled with deionized water and set to the desired test temperature, allowing sufficient time for temperature stabilization. Each nanofluid sample was thoroughly dispersed before measurement and transferred into a clean beaker. The beaker was placed within the temperature-controlled bath to maintain the target temperature during testing. The viscometer was powered on, auto-zeroed, and fitted with the appropriate spindle selected according to the expected viscosity range of the sample. The spindle was fully submerged to the immersion mark without contacting the beaker walls or base, and care was taken to avoid entrapping air bubbles. Once the sample temperature stabilized, viscosity measurements were recorded at the selected spindle

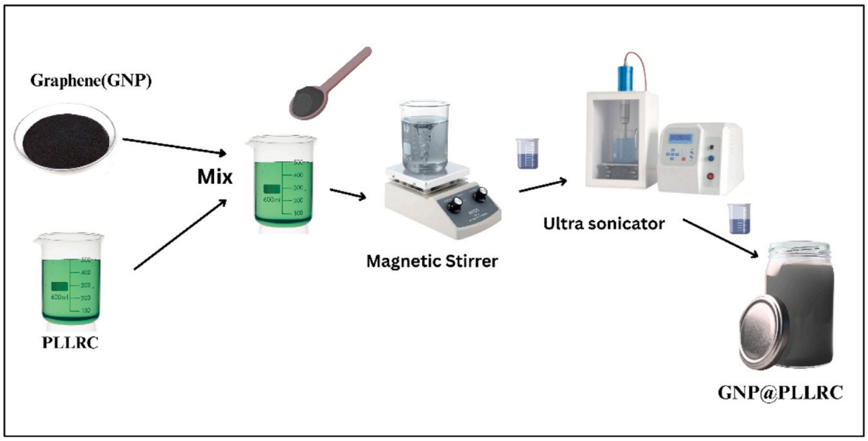

Fig. 3. Synthesis of GNP@ PLLRC.

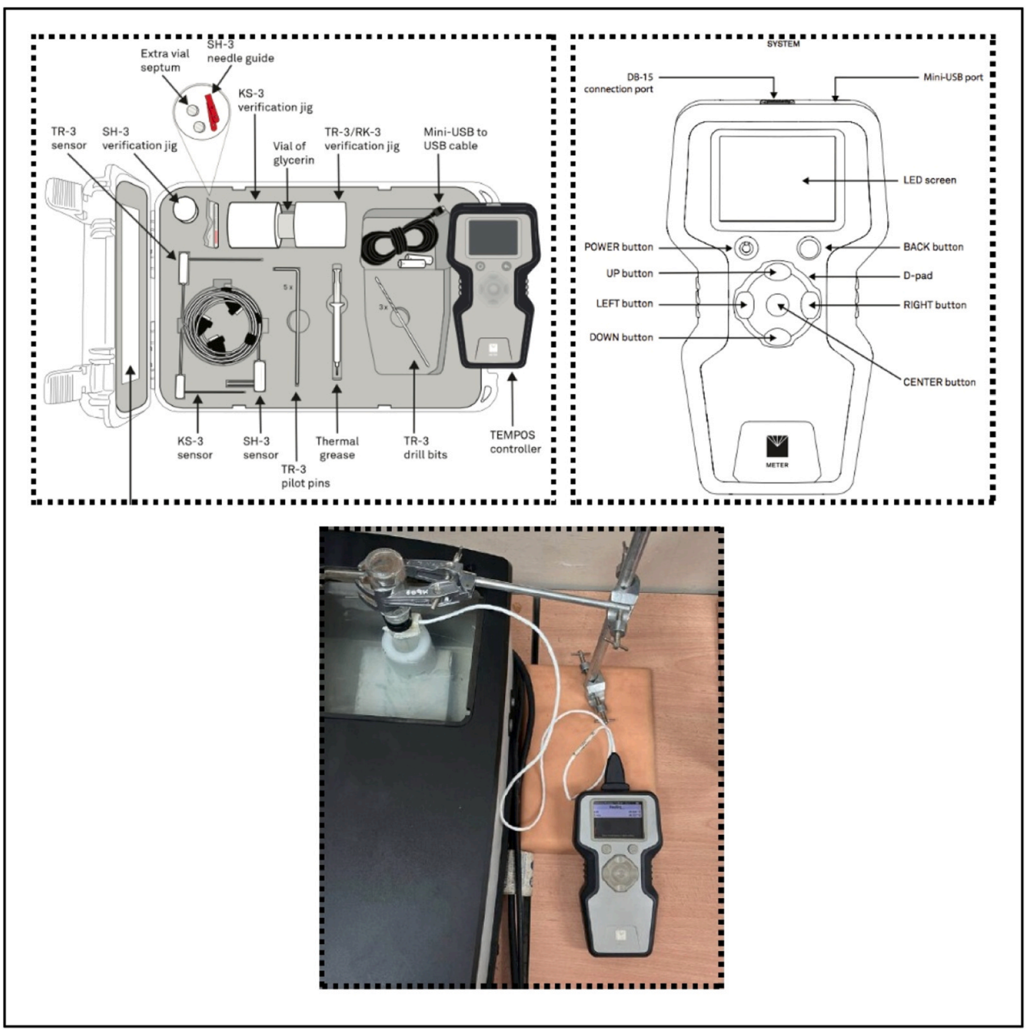

Fig. 4. Meter© Tempos thermal properties analyzer.

speed. Fig. 5 shows the functional part of the viscometer. The procedure was repeated for all test temperatures and concentrations. Between measurements, both the spindle and beaker were thoroughly cleaned and dried to prevent contamination. All measurements were performed under identical environmental and operational conditions to ensure repeatability and accuracy.

2.7. *Experimental setup for performance evaluation*

The performance evaluation of GNP@PLLRC nano fluids was carried out using a Perodua Kancil cooling system following standard procedures for consistency and safety. The required amount of nanofluid was poured into the water tank, with an immersion heater and thermocouple

Fig. 5. Brookfield Viscometer DV III ultra with TC550 water bath.

placed inside before sealing the lid. The temperature controller was switched on, and the desired temperature was set. Once the set temperature was reached and the heater switched off, the main valve was opened, and the water pump and blower fan were activated to simulate actual operating conditions. A USB cable connects the Arduino system to a laptop for data logging with PLX-DAQ. The pump voltage is adjusted to control the fluid flow rate. The graphene nanofluid circulates through the radiator pipes while the system fan runs to simulate real operating conditions. Cyclic tests are performed for each nanoparticle concentration, running the system for 30 min and 1 h to evaluate heat dissipation and contamination. After each test, all equipment is switched off and the coolant is fully drained. Fig. 6 shows the functional part of test rig. For different graphene concentrations, all setup, calibration, and testing steps are repeated to ensure consistent conditions. Calibration of flow meters, temperature sensors, and pressure gauges is done as needed. After testing, data from sensors and the RS485-controlled stepper motor are analyzed, with maintenance and troubleshooting carried out as per safety and reliability standards.

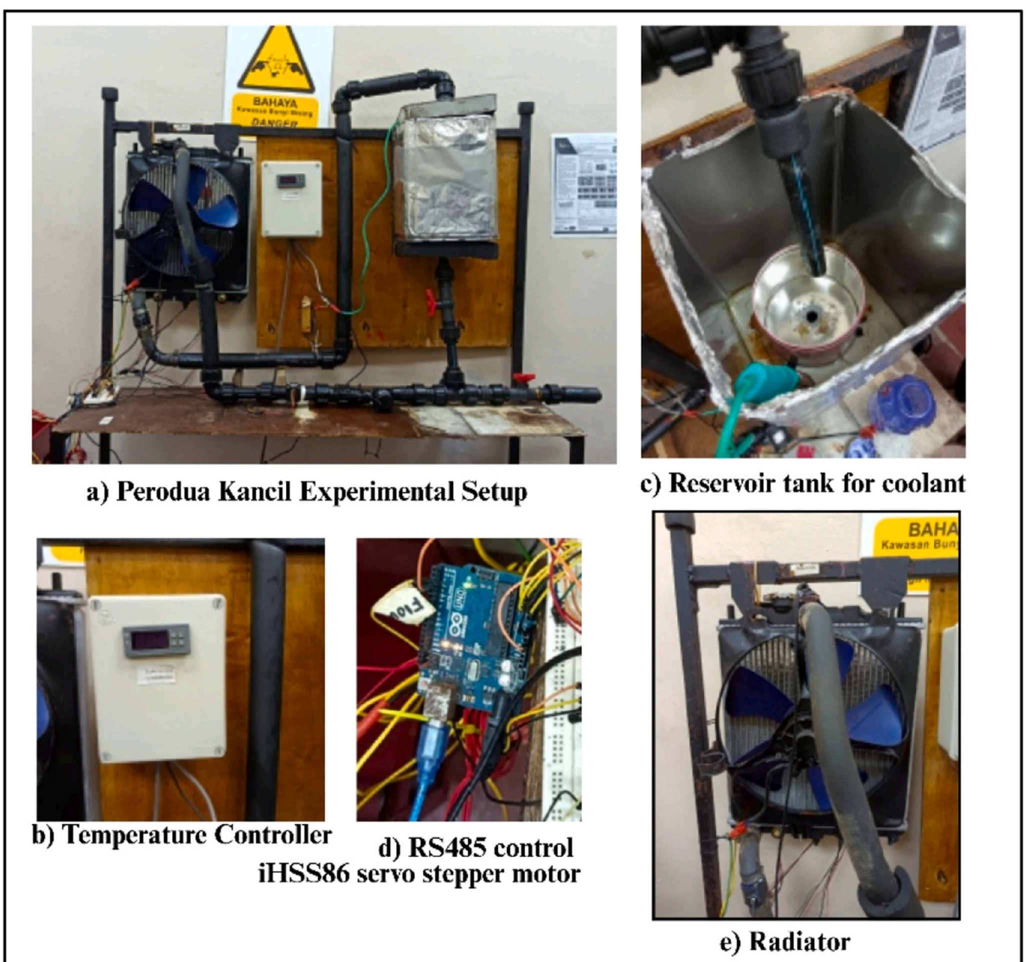

Fig. 6. Functional parts of Perodua Kancil experimental setup.

2.8. Radiator exhaust temperature measurement and analysis

The outlet temperatures of the Perodua Kancil automotive cooling system were measured for three coolant types at the highest test concentration (0.09 wt%): pure PLLRC base fluid, GNP@PLLRC nanofluid, and contaminated GNP@PLLRC nanofluid. Measurements were conducted at inlet temperatures ranging from 30 °C to 70 °C to evaluate cooling performance under varying thermal loads. Temperature evaluation was performed using an infrared camera FLIR E4 because of the non-contact measurement benefit that minimizes error of measurement that is common with thermocouples or contact probes. The FLIR E4 has an infrared sensor of 80 × 60 pixels and MSX® image enhancement technology which allows the camera to perform quality and precise thermal imaging. The FLIR E4 is portable and robust as it has a thermal sensitivity of 0.15 °C which is shown in Fig. 7 and has a 45 °FOV with a 0.5 m of minimum focus distance. The FLIR E4 camera has a 3.0 in. color LCD screen of 320 × 240 pixels and has several image mode options of thermal and MSX to increase visualization. The camera has an automatic operation and focus free which is powered by a rechargeable Li-ion battery which allows 4 h of utilization. The FLIR E4 has USB port for data reading and has a temperature measurement range of −20 °C to 250 °C with a measurement error of 2 °C. The camera is also designed to provide reliable performance in extreme temperature conditions so that it can provide thermal measurement data accurately. Fig. 7 shows the thermal imaging camera. For each test condition, the coolant was circulated in the engine cooling system until the desired inlet temperature stabilized. The FLIR E4 was then positioned at a fixed distance and angle relative to the radiator outlet to capture thermal images. Multiple readings were taken to ensure consistency, and the mean outlet temperature was used for analysis. The inclusion of 0.09 wt% GNP in the PLLRC base fluid was expected to enhance thermal conductivity and overall heat transfer performance. The contaminated GNP@PLLRC nanofluid was tested to determine the effect of impurities on cooling efficiency. Comparative analysis of outlet temperatures across the three coolant types provided insight into the thermal performance improvements achievable through nanoparticle addition, as well as the potential degradation caused by contamination.

3. Results

Graphene nanofluids, known for their superior thermal properties, are studied at varying concentrations (0.01–0.09 wt%) to assess heat transfer performance. Techniques like SEM, EDX, XRD, UV-Vis, FTIR, and tests for thermal conductivity and viscosity are used to link GNP with PLLRC to an experimental study of the solutions' behavior. Fig. 8 shows the visual appearance of nanofluid after two weeks

3.1. Surface & composition analysis of nanoparticle

3.1.1. Scanning electron microscopy coupled with energy dispersive X-ray (SEM/EDX) spectroscopy

The SEM is carried out on a JEOL JSM-IT200 floor-top SEM machine

Fig. 7. FLIR E4 Infrared Camera.

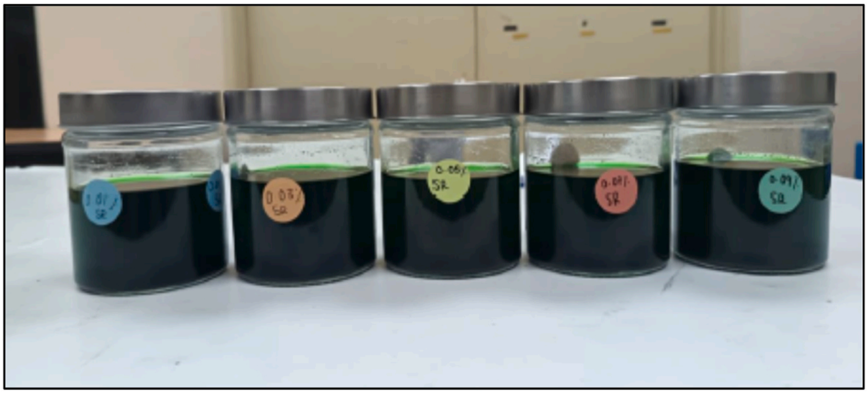

Fig. 8. Visual appearance of GNP@PLLRC after 14 days.

with up to 30,000X magnification and built-in EDX. SEM images and EDX analysis of the graphene nanoparticles reveal that highly promising material for coolant enhancement. With reference to the Fig. 9 At low magnification (100x), the SEM shows thin, irregular graphene flakes with a loose, layered structure, indicating few to multi-layer sheets with significant surface area. At higher magnification (2,000x), the flakes appear wrinkled with pointed edges, underscoring their ultrathin, plate-like form and rough surface, which should enhance them disperse well in coolant. This structure also maximizes contact with the coolant base fluid, likely improving heat transfer. The EDX data confirms the flakes are mostly pure carbon (98.6%) with minimal oxygen (1.4%), reflecting high chemical purity and slight oxidation, ideal for maintaining graphene's conductivity while aiding dispersion. No significant contaminants or metals are seen, ensuring stability and corrosion resistance. Overall, these graphene flakes combine large surface area, crumpled morphology, and high purity to offer efficient heat dissipation and potentially longer coolant life when used in PLLRC.

3.2. *Crystallographic analysis*

3.2.1. *X-ray diffraction (XRD)*

XRD patterns were recorded on a PANalytical X'Pert[3] diffractometer using Cu Kα radiation ($\lambda = 1.54184$ Å) over an angle range 3°–150°. Crystallite size D was estimated from the Scherrer equation [50], representing Eq. (1),

$$\boldsymbol{D} = \frac{K\lambda}{\beta\cos\theta} \tag{1}$$

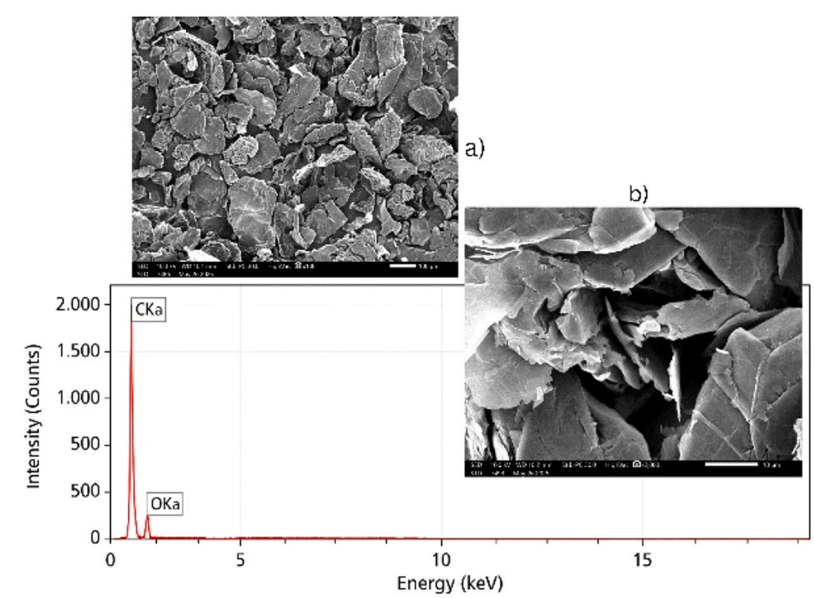

Items	Value	Display name		Standard data	Quantification metdhd	Result Type
measurement conditions		Spc_005		ZAF	Quantification	Metal
Acceleration voltage		Element	Line	Mass.	Mass%	Atom%
Probe current		C	K		98.40 ± 0.51	98.80 ± 0.51
Magnification	x 1000	O	K		1.60 ± 0.23	1.20 ± 0.17
Measurement director	First	Total			100,00	
Live time	30.0 sec					Fitting ratio 0,068
Deal time	20.21 sec					
Count rate	32.0%					
Count rate	555.00 CPS					

Fig. 9. SEM images of Graphene a) at 100X and b) 2000X magnification along with EDX analysis of graphene.

with K= 0.9 K= 0.9, where β is the FWHM and θ the Bragg angle.

With reference to Fig. 10, X-ray diffraction (XRD) analysis of the graphene sample shows a strong, sharp peak at 2θ ≈ 26.51° (d = 3.36 Å), matching the (002) plane of reference graphite 2 H (hexagonal, a = 2.464 Å, c = 6.711 Å, space group P63/mmc) [51]. This peak, with high intensity (44,003 counts) and narrow FWHM (~0.3°), indicates well-ordered graphitic layers typical of multilayer graphene. The crystallite sizes (252–270 Å) and low micro strain (0.62–0.36%) further confirm large, ordered domains with minimal defects. Additional weak peaks are seen at 42.44°, 43.75°, 44.80°, 54.63°, and 77.55°, corresponding to the (100), (101), (004), (110), and (112) planes of hexagonal graphite [52]. Their low intensity and broadening indicate limited stacking order and reduced layer coherence, typical of exfoliated or few-layer graphene [53]. The peak positions closely match the reference (Graphite 2 H, C1), with shifts below 0.2°(2θ), confirming phase identification and minimal lattice distortion. Weak secondary peaks and their relative sharpness indicate hexagonal symmetry and a lack of significant impurities. Overall, the XRD pattern reveals a well-ordered, graphitic few-layer graphene with large crystallites, high phase purity, and minimal disorder closely resembling pure graphite but with features consistent with synthetic few-layer graphene or nanoplatelets.

3.3. Spectroscopic analysis of nanofluids

3.3.1. Fourier Transform Infrared Spectroscopy (FTIR)

The FTIR was carried out on a Thermofisher Scientific Nicolet iS50 machine, which is capable of the mid-to-far IR range of 600–4000cm-1. As per the Fig. 11 comparative FTIR diagram, the original coolant's spectrum mainly shows ethylene-glycol bands. Adding 0.01–0.09 wt% graphene preserves these bands but adds new lattice/π–π features (Appx 518–640 cm^{-1}) and weakens O–H and C–O stretches, suggesting glycol physically adsorbs onto graphene with some hydrogen-bond changes, not new covalent bonds. The FTIR comparison of PETRONAS Long-Life Radiator Coolant (PLLRC) with graphene-enhanced variants (0.01–0.09 wt%) shows that ethylene glycol remains the dominant component (similar 83.4–83.5%). The largest changes appear in the O–H stretching band (3200–3600 cm^{-1}) which is critical for understanding hydrogen bonding networks and intermolecular interactions. A intense absorption band centered at 3335.33 cm^{-1} indicates extensive hydrogen bonding among hydroxyl groups from water and glycol molecules. from 0.01% to 0.07% GRP, transmittance steadily decreases by 8.6–13.9%, indicating stronger hydrogen bonding between graphene and glycol hydroxyls. This reduction in transmittance indicates stronger

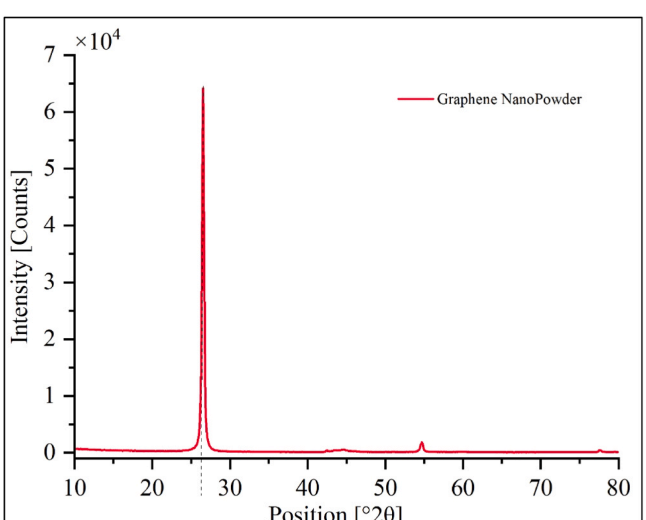

Fig. 10. XRD pattern of GNP.

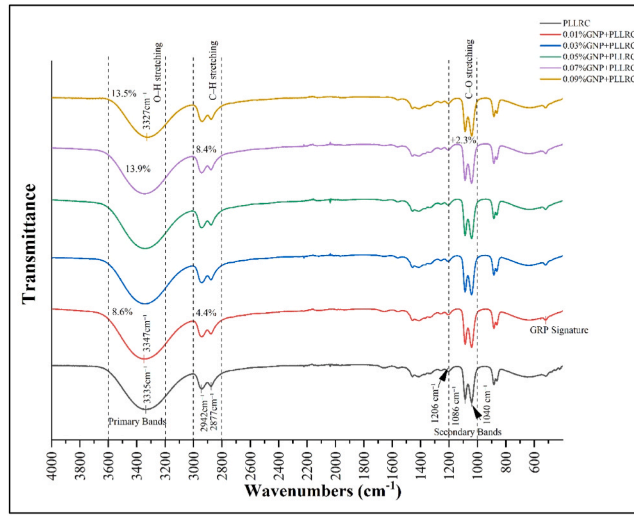

Fig. 11. FTIR comparative pattern of nanofluids.

molecular associations, likely due to the high surface area of graphene facilitating multiple interaction sites with the hydroxyl groups of ethylene glycol through hydrogen bonding and surfactants [54]. At 0.09%, transmittance jumps by 13.5%, implying nanoparticle aggregation that limits available surface area and alters interactions. In the C–H stretch region (2800–3000 cm^{-1}), two distinct peaks at 2942 cm^{-1} and 2877 cm^{-1} confirm the presence of saturated aliphatic chains characteristic of polyglycol structures. GRP loadings up to 0.07 wt% cause a steady transmittance drop of 4.4–8.4% (largest at 0.07 wt%), showing graphene's effect on aliphatic C–H bonds—likely via π–π stacking with the coolant's hydrocarbon regions. At 0.09 wt%, this change falls to –0.4%, pointing to nanoparticle aggregation and reduced surface interactions. In contrast, the C–O stretch band (1000–1200 cm^{-1}) in which The base fluid shows a characteristic triple-peak pattern at 1206, 1086, and 1040 cm^{-1} in which variation only –1.5% to + 2.3% with no concentration trend despite nanoparticle addition. This preservation of the C-O bonds is crucial for maintaining the coolant's fundamental properties while benefiting from the enhanced characteristics imparted by the nanoparticles. In the fingerprint region (400–1500 cm^{-1}), GRP additions cause only slight increases in transmittance (+0.3% to +2.0%). Spectral changes peak nonlinearly at 0.01–0.07 wt%, where well-dispersed nanoparticles interact via hydrogen bonding, π–π stacking, surface adsorption, and possible ordered interfacial layers. At 0.09 wt%, a critical threshold where the benefits of increased surface area are counteracted by nanoparticle agglomeration, leading to reduced dispersion stability and altered interaction patterns, aggregation reduces these effects, marking a threshold common in nanofluids. FTIR thus pinpoints 0.01–0.07 wt% as the optimal GRP range for enhanced molecular interactions and, by extension, improved thermal and flow properties without altering the coolant's fundamental structure.

3.3.2. UV-Vis

The UV–Vis absorbance spectra of graphene nanoparticle (GNP) dispersions in Petronas Long-Life Radiator Coolant (PLLRC) demonstrate clear, concentration-dependent optical behavior. As GNP content increases from 0.01 wt% to 0.09 wt%, absorbance intensifies across the UV–visible range, exhibiting marked light–substance interactions. At lower concentrations (0.01–0.03 wt%), absorbance remains modest and primarily reflects the chromophoric activity of the PLLRC base fluid. Above 0.05 wt%, absorbance rises sharply, commonly going beyond the spectrophotometer's upper detection limit (5.0 a.u.) at wavelengths above 308 nm, which suggests complete photon attenuation due to photon absorption and scattering. The observed deviation from linearity indicates significant interparticle interactions along with optical coupling, characteristic of stable graphene nanofluids. The most pronounced absorbance increase takes place in the visible region (420–700 nm), where 0.07 wt% GNP achieves 2.2–3.6 a.u. before saturation. These results identify 0.05–0.07 wt% as the optimal concentration range, balancing improved thermal conductivity with minimal viscosity increase to preserve stability and pump efficiency. The absence of anomalous optical features confirms that GNP addition does not affect PLLRC's physicochemical properties, including thermal capacity, corrosion inhibition, and viscosity index. Consistent peaks at 420 nm and 480 nm indicate minimal particle agglomeration, uniform dispersion, and strong nanoparticle–fluid interphase interactions. Overall, the findings show that precise GNP loading controls the optical, rheological, and thermophysical properties of PLLRC-based nanofluids. These results correspond with prior studies on graphene-enhanced heat transfer fluids and support their use in advanced automotive cooling and energy management applications. Fig. 12 showing various comparative UV-Vis diagram of nanofluids.

3.4. Thermal conductivity analysis of nanofluid

In engine cooling applications, maximizing thermal conductivity is essential for efficient heat dissipation and stable engine performance. Increasing GNP concentration significantly enhances the composite's thermal conductivity, enabling faster heat removal and improved thermal management. The graph shows that increasing graphene nanoparticle concentration significantly boosts the thermal conductivity of nanofluids, especially as temperature rises from 30°C to 70°C. Fig. 13 shows the variation of thermal conductivity with temperature at different concentration. The base fluid without nanoparticles has the lowest thermal conductivity (0.108 W/mK) and slowly increases to 0.158 W/mK@70°C. Even with just 0.01% GNP, conductivity improves, and this effect grows stronger at higher concentrations [55]. The observed enhancement in thermal performance is attributed to a synergistic effect by which particle concentration and Brownian motion are linked. The frequency of stochastic motion within the fluid is intensified by a higher number density of nanoparticles as the graphene concentration is increased. Micro-convection—a micro-stirring effect by which the fluid boundary layers around the nanoparticles are disturbed. It is induced by Brownian motion. Furthermore, this mechanism is amplified by the kinetic energy of the particles; stronger localized convection currents are created by the intensified Brownian motion as temperature rises, whereby the base fluid is effectively mixed at the nanoscale. Consequently, thermal resistance is significantly reduced by the combination of increased particle density and micro-convection, whereby the upward trend in thermal conductivity shown in Fig. 13 is driven. At

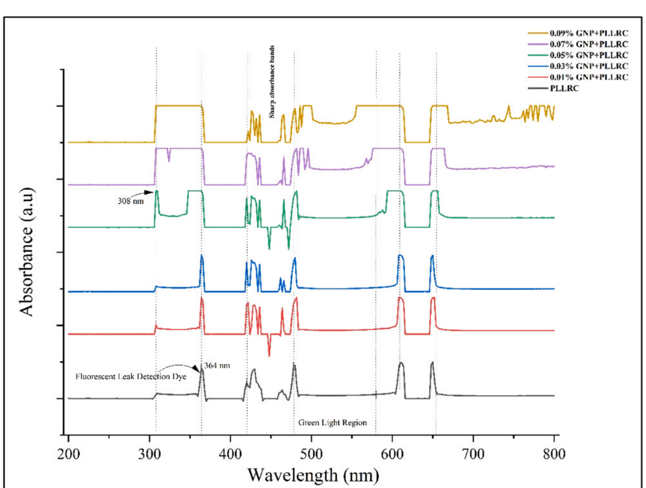

Fig. 12. UV–vis comparative pattern of nanofluids.

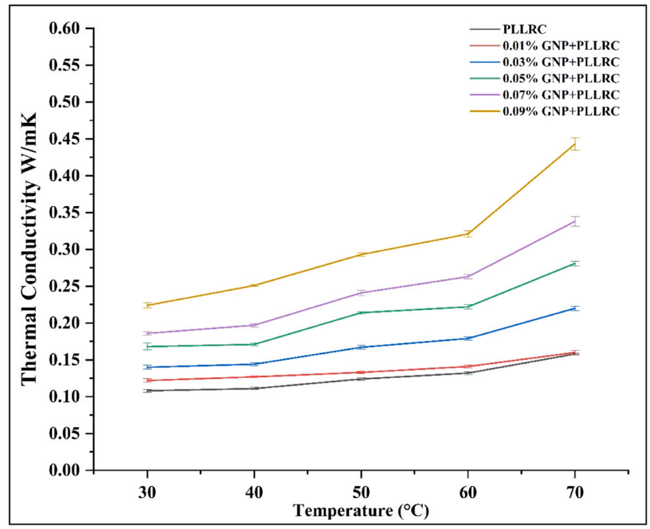

Fig. 13. Thermal conductivity of PLLRC and GNP–PLLRC at 30–70ºC.

0.09% graphene show the highest thermal conductivity 0.443 W/mK@70°C, the improvement is dramatic, especially at higher temperatures, likely due to intensified Brownian motion and better thermal pathways within the fluid [56]. The results highlight how combining higher graphene levels with elevated temperatures can create nanofluids with superior heat transfer abilities, making them ideal for advanced cooling in electronics, automotive, and industrial systems [57]. Properly adjusting graphene content and temperature can tune nanofluid performance far beyond conventional coolants.

3.4.1. Uncertainty analysis of thermal conductivity

The experimental thermal conductivity (K) data for nanofluid samples, the base fluid PLLRC, and the 0.01% GNP+PLLRC nanofluid samples were consistent and showed low random uncertainty. the analysis was performed by assessing the repeatability of five obtained measures (set 1 to set 5) for each concentration and temperature point taken. This included the standard deviation (S) and the standard error of the mean ($U_{\bar{x}}$). The standard deviation, indicating data spread, was extremely low, between 0.002 and 0.010 W/mK. The standard error of the mean, the primary metric of random experimental uncertainty, was then determined to be ±0.002 to ±0.008 W/mK. For thermal conductivity, then, expressed as relative uncertainty (%U), the overall experimental measurements sources of experimental error showed that a maximum uncertainty of 1.83% was in fact registered by this 0.01% GNP+PLLRC sample at 30°C, and a minimum 0.67% was obtained from the base fluid at 70°C. This low relative uncertainty across the region indicates that the experimental method was reliable and highly repeatable, with all measurements falling well within the typical ±2.0% tolerance for high-quality thermal conductivity measurements in fluid systems.

3.5. Rheological (Dynamic viscosity) analysis of nanofluid

High thermal conductivity is necessary for proper engine cooling, while proper viscosity maintains smooth coolant flow and lowers pumping power. Excessive viscosity increases flow resistance and energy loss. The moderate viscosity of GNP-enhanced PLLRC indicates it can improve heat transfer without impairing circulation efficiency, considering it a viable candidate for engine cooling. The Brookfield DV III Ultra Viscometer measures the dynamic viscosity of fluids such as PLLRC with GNP using a rotating spindle and digital display for accurate, repeatable results. The TC 550 Laboratory Water Bath ensures consistent temperature control, essential for precise viscosity measurements. Together, they provide reliable analysis of coolant nanofluids under controlled lab conditions. The viscosity measurements were performed using a Brookfield DV III Ultra Viscometer with a rotating spindle and digital display, ensuring accurate and repeatable results. The TC 550 Laboratory Water Bath provided stable temperature control, with a range from −20°C to 135°C and high stability (±0.07°C), essential for precise viscosity analysis. Each sample was measured at least twenty times, and the average value was used for reliable analysis under controlled lab conditions [58]. Fig. 14 shows the variation of viscosity with temperature and concentration. Across all samples, viscosity decreases as temperature rises, consistent with typical liquid behavior. The impact of graphene nanoparticles is strongest at lower temperatures; for example, at 30°C, pure PLLRC averages 10.87 cP, increases to 16.21 cP at 0.07 wt% GNP, but drops to 8.18 cP at 0.09 wt%. This trend continues at higher temperatures (at 70°C, PLLRC is 3.16 cP, 0.07 wt% GNP is 7.07 cP, but 0.09 wt% falls to 2.33 cP), showing that too much GNP lowers viscosity, especially when hot [59]. Thus, adding GNP up to about 0.07 wt% maximizes viscosity, while higher concentrations reduce it due to factors such as particle aggregation, informing the optimal coolant formulation for thermal performance.

3.5.1. *Uncertainty analysis of nanofluid viscosity*

The viscosity (μ) values of the experimental nanofluid sample, measured across different temperatures and concentrations, were free of any pronounced random uncertainty. This is because at each data point, twenty (N = 20) measurements were made with very high repeatability. The standard deviation (S) and the standard error of the mean ($U\bar{\mu}$) were two indices for assessing repeatability. Usual precision, the standard deviation of data, was generally within points around 0.01 cP and 0.11 cP; in turn, this brought about an extremely low standard error of the mean, $U\bar{\mu}$, on the order of ±0.002 cP to ±0.008 cP. The U_{total} had a main contribution from U_{sys}, due to the Brookfield DV-III Viscometer 's precision of ±1% FSR, causing it to vary anywhere from within 0.5–2 cP. In terms of relative uncertainty (%U), the total experimental error was as follows: for samples with data at 25 per cent of the FSR, it was around 4.0%, but for those with about 100 per cent FSR U in relative finally did not exceed 1.0%. These results show that while the experimental method used in this study is extremely stable and has been repeated many times, the choice of speed range and measuring point is very critical in ensuring maximum accuracy.

3.6. *Radiator exhaust temperature analysis*

A GNP concentration of 0.09 wt% was selected for its optimal dispersion stability, viscosity control, and maximum thermal conductivity enhancement. Higher concentrations caused particle agglomeration and increased viscosity, while lower concentrations provided less thermal improvement. Therefore, 0.09 wt% is the most reliable and effective composition for heat transfer in engine cooling applications. Compared measured temperatures for PLLRC base fluid, 0.09% graphene +PLLRC nanofluid (GNP+PLLRC), and contaminated nanofluid (0.09% GNP+PLLRC(c)) as inlet temperatures rise from 30 °C to 70 °C. Fig. 15 showing the variation of temperature profile of radiator at higher concentration in between the 30 min time interval. All fluids show a linear increase in outlet temperature with higher inlet values. The PLLRC base fluid consistently has higher outlet temperatures, showing it is less efficient at heat transfer. In contrast, the 0.09% GNP+PLLRC, especially at 50 °C, exits at lower temperatures, indicating better heat removal and superior thermal conductivity from the graphene nanoparticles [60]. The contaminated 0.09% GNP+PLLRC(c) shows unusual behavior, its outlet(final) temperature is similar to or higher than the base fluid at 30 °C and 70 °C, but outperforms both fluids at 50 °C, suggesting a peak in thermal performance [61]. This may be due to changes in nanoparticle distribution caused by contaminants but also highlights the unpredictability such contamination brings to cooling applications [62].A comparative temperature graph was plotted to know the cooling performance of the radiator as shown in Fig. 16.Across the full temperature range, the 0.09 GNP+PLLRC nanofluid shows the strongest cooling performance. It showing the contaminated 0.09 GNP+PLLRC(c) generally second and the base PLLRC least effective, indicating that adding 0.09% graphene nanoparticles clearly enhances radiator heat transfer. Table 2 shows the reduction percentage in temperature at different operating temperatures. At 30 °C, the percentage temperature drop over 30 min is about 6.82% for 0.09 GNP+PLLRC, compared with 2.63% for PLLRC and 1.64% for 0.09 GNP+PLLRC(c). It shows the fresh graphene nanofluid cools roughly 4–5 %age points more than the base fluid. At 40 °C, the reused nanofluid gives the highest drop (about 10.4%), slightly above the fresh GNP nanofluid (9.69%) and clearly above PLLRC (7.88%), indicating that even after prior radiator use and some contamination, the graphene-containing coolant still outperforms the base fluid. The most pronounced improvement occurs around 50 °C, where 0.09 GNP+PLLRC shows a 20% reduction in temperature compared with about 10% for PLLRC and 12.2% for 0.09 GNP+PLLRC(c). Therefore, the fresh nanofluid nearly doubles the cooling effectiveness relative to the base coolant at this condition. At higher temperatures of 60–70 °C, all three fluids show larger drops, but 0.09 GNP+PLLRC generally maintains a small advantage (about 0.5–2.5 %age points higher cooling than PLLRC), while the reused nanofluid remains between the base fluid and the fresh GNP nanofluid, confirming that graphene nanoparticles enhance radiator cooling efficiency and that this benefit persists, though reduced, when the nanofluid is reused.

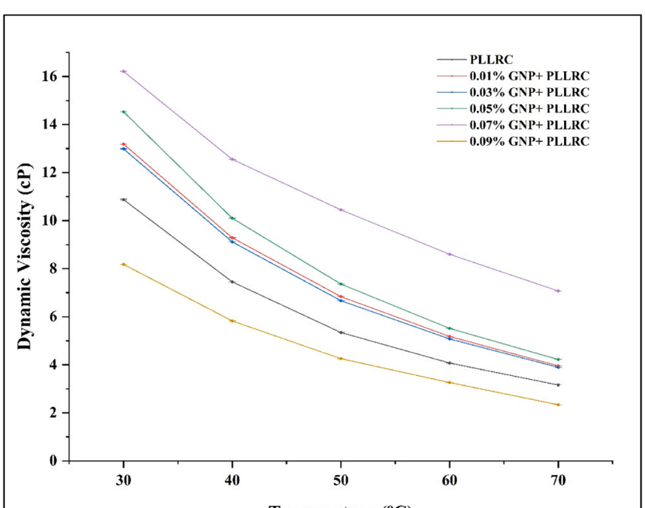

Fig. 14. Dynamic viscosity of PLLRC and GNP–PLLRC at 30–70°C.

4. Discussion

Due to the elevated thermal conductivity of all tested concentrations, the concentration at 0.09 wt% for graphene nanoparticles (GNPs) dispersed in PLLRC was selected. A significant improvement in thermal performance was obtained at this concentration which optimized the - nanofluid heat transfer capacity and determined it as an ideal candidate for the study of contamination effects after use in operating conditions. The procedure comprised the introduction of a 30-minute operational cycle representative of service conditions for the 0.09 wt% nanofluid, so that the suspension could be sized with respect to wear debris, chemical degradation products, and agglomerates of nanoparticles. This generates a more realistic post-operation state with respect to the thermal and r-heological changes that the coolant undergoes, and this data provides insight into how performance degrades during actual automotive cooling applications. Thus, the generated nanofluid is referred to as a contaminated nanofluid 0.09% GNP+PLLRC(c). In summary, clean 0.09% GNP+PLLRC improves heat transfer by lowering outlet temperatures, while the base fluid is less efficient. Erratic patterns for

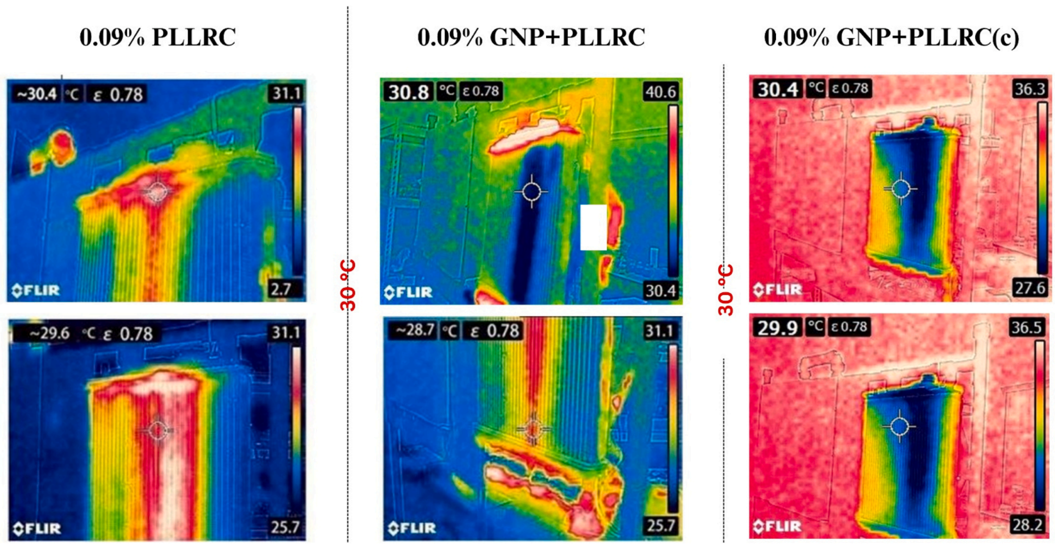

(a)

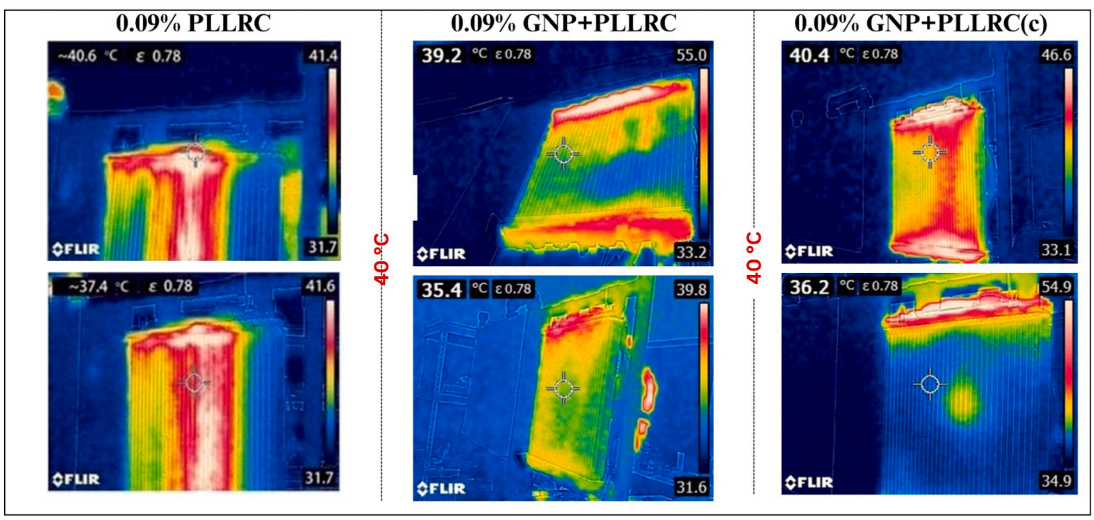

(b)

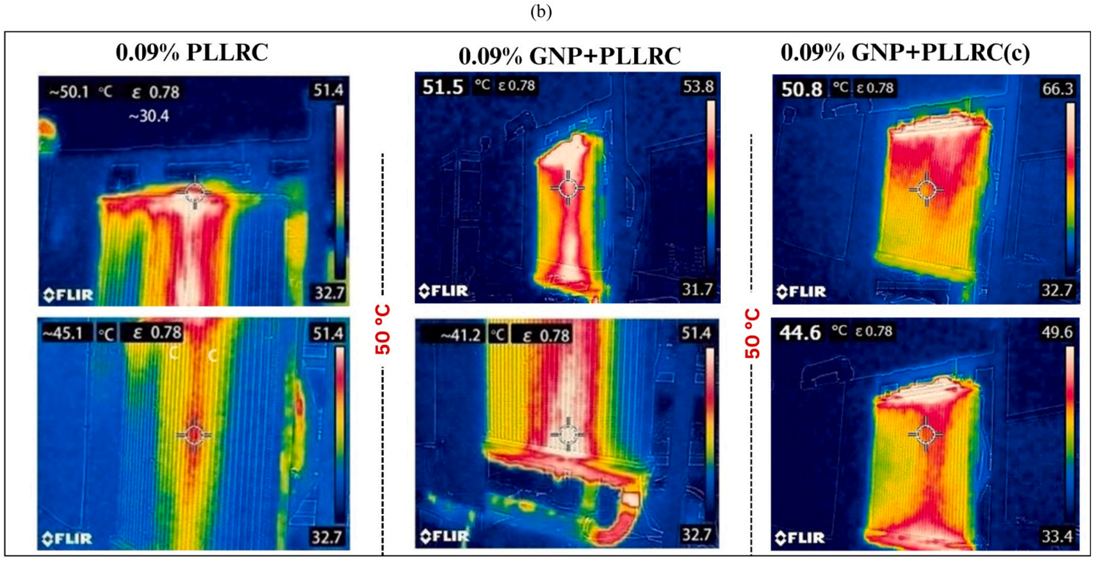

(c)

Fig. 15. a),b),c),d),e) Radiator thermal images of PLLRC, fresh and contaminated 0.09% GNP-PLLRC 30–70ºC over 30 min.

thermophysical properties are also exhibited by contaminated nanofluids because contaminants can affect the dispersion of

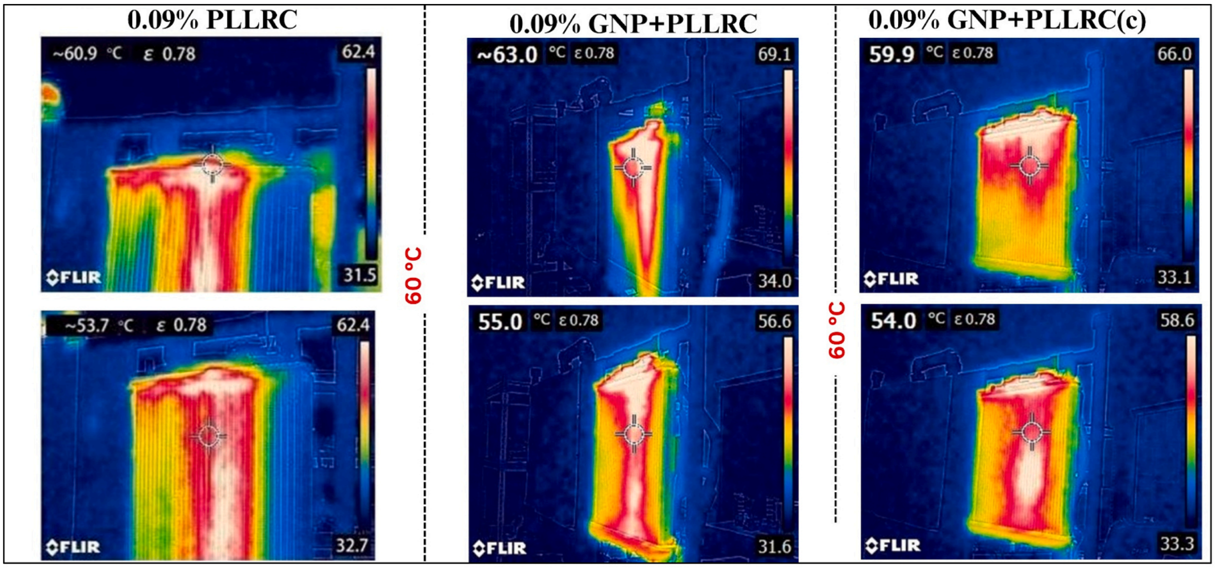

(d)

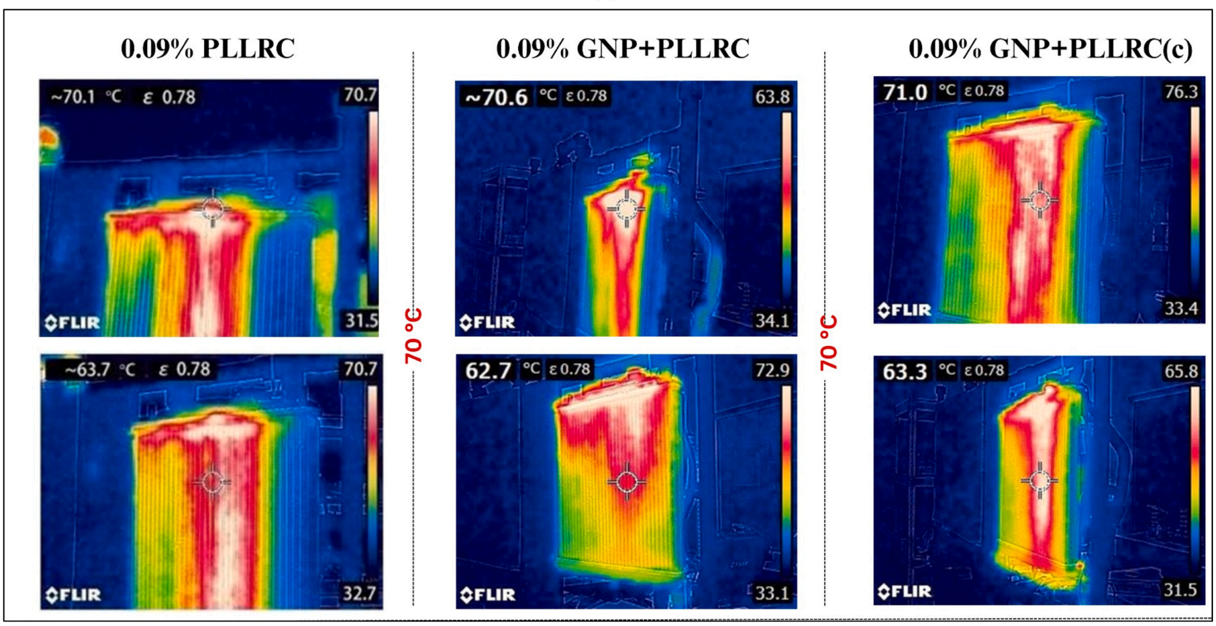

(e)

Fig. 15. (*continued*).

nanoparticles and modify the stability of thermodynamic surfactants, leading to unpredictable thermal behaviors. One of the major contributors is the net agglomeration of nanoparticles, which leads to flow obstruction, increased viscosity, and lower thermal conductivities, thereby degrading temperature-dependent heat transfer efficiencies. Moreover, modifications of surfactants used to stabilize nanofluids can promote thermal stratification by self-destabilizing suspensions and leading to a granular poorly distributed arrangement of non-dispersed heat transfer fluids (HTF). Within a temperature window around 50 °C, there might be a momentary vigorous dispersive interaction by nanoparticles within the base fluid leading to improved thermal conductivities and heat transfer enhancement. However, above this temperature the stability drops leading to clustering of nanoparticles and thermal performance even worse than the base fluid. Such behavior in contaminated nanofluids is a reminder of the importance of dispersive stability of nanoparticles and thermos-modulating surfactants for reliable performance. Fig. 17 showing the temperature driven heat transfer behavior of nanofluid.

Graphene nanofluids offer superior thermal characteristics for use in automotive cooling systems but necessitate greater pumping power owing to the higher viscosity of the fluids at greater concentrations. Nonetheless, viscosity tends to decrease at higher temperatures and, at temperatures in the operational range of 30–70°C, effects are more acceptable when the concentrations are kept within 0.03–0.09 wt%. Most industrial-purpose pumps, including centrifugal pumps, are designed to function optimally in these viscosity ranges. This operational condition allows the pumps to be easily incorporated in the existing cooling circuits. The type of surfactant used also has a significant influence on the corrosion characteristics of the nanofluids. Surfactants like GA, SDS, and Tween 80 are known to reduce the corrosion of the copper constituent in the radiator, while some surfactants like SDBS may aggravate the corrosion problem [63,64]. For the more durable materials to be used in the system to be kept intact, the surfactant systems must be judiciously formulated, and the system has to be kept

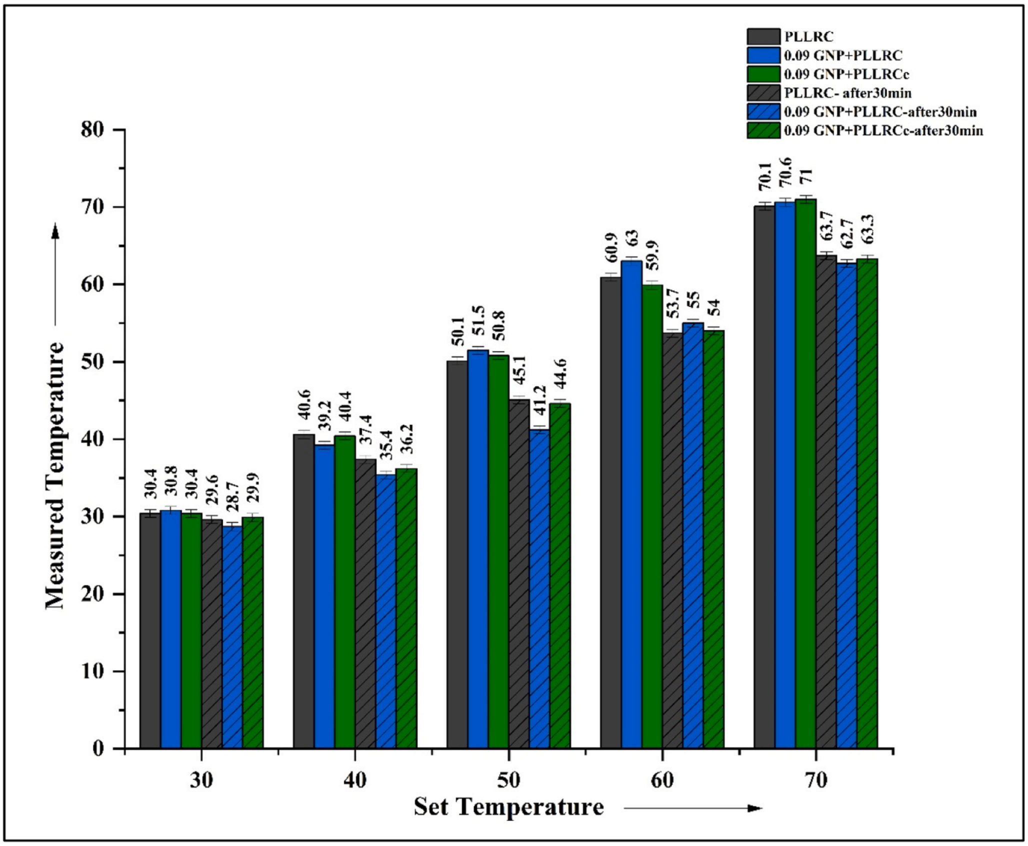

Fig. 16. Test rig set vs measured temperature for PLLRC, GNP+PLLRC, and GNP+PLLRC(c).

Table 2
Temperature reduction % of coolant at set temperatures in 30 min intervals.

Temperature °C	PLLRC	Temperature °C	0.09 GNP+PLLRC	Temperature °C	0.09 GNP+PLLRCc
30	2.63%	**30**	6.82%	**30**	1.64%
40	7.88%	**40**	9.69%	**40**	10.40%
50	9.98%	**50**	20.00%	**50**	12.20%
60	11.82%	**60**	12.70%	**60**	9.85%
70	9.13%	**70**	11.19%	**70**	10.85%

clean. For sustained performance, the maintenance intervals in the nanofluid systems must be well considered. The stability and effectiveness of the nanofluids in the maintenance of stable dispersion of the nanoparticles and efficient dispersion of energy in the system against contamination. Regular filtration and periodic replacement are recommended to prevent issues such as nanoparticle agglomeration or sedimentation, particularly in demanding automotive environments.

5. Conclusions

This experimental process demonstrates that adding graphene nanoparticles to car coolant fluids significantly improves their thermophysical properties, enhancing thermal management in automotive radiators. The main improvement was a significant boost in thermal conductivity, leading to better heat dissipation during engine use. This is crucial for modern, compact engines with higher power, which can quickly overheat. By improving heat transfer, graphene nanofluids may extend engine lifespan and enhance performance stability under tough conditions. Optimal thermophysical performance was achieved at 0.09% graphene, beyond which no further benefits were observed, and stability issues arose. Viscosity remained within desirable limits for automotive systems, preventing efficiency loss. Advanced analyses (FTIR, XRD, SEM, UV–VIS, TGA) confirmed good dispersion, structural stability, and the reproducibility of the nanofluids. A key aspect of this study is its examination of how real-world contaminants like engine oil, rust, and dirt affect graphene-enhanced coolants. Tests showed that such impurities reduce both thermal conductivity and heat removal efficiency.

The major findings on thermal conductivity, viscosity, and temperature analysis are as follows.

- Thermal conductivity increases steadily with temperature for all fluids, rising from 30 °C to 70 °C. For example, PLLRC base fluid (BF) increases from 0.108 W/m·K at 30 °C to 0.158 W/m·K at 70 °C.
- At every temperature, graphene nanofluids (GNP+PLLRC) show higher thermal conductivity than the base PLLRC. At 30 °C, K increases from 0.108 W/m·K (BF) to 0.224 W/m·K at 0.09 wt% GNP, nearly doubling the base value. At 70 °C, K increases from 0.158 W/m·K (BF) to 0.443 W/m·K at 0.09 wt% GNP, achieving nearly a threefold enhancement.
- Dynamic viscosity decreases steadily with temperature for all fluids, from 30 °C to 70 °C. For example, PLLRC base fluid drops from 10.87 cP at 30 °C to 3.16 cP at 70 °C.

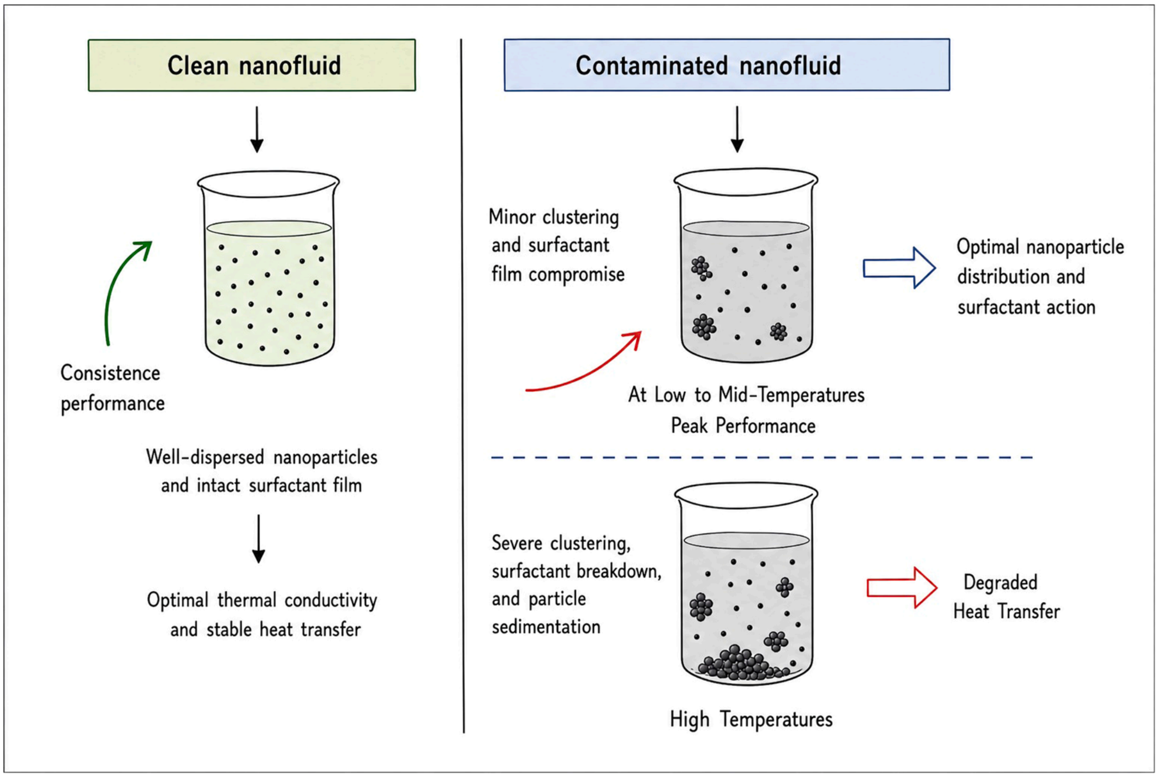

Fig. 17. Temperature-driven heat-transfer behavior of clean versus contaminated nanofluids.

- At 30 °C, adding graphene increases viscosity for most concentrations (0.01–0.07 wt% GNP: 13.19–16.21 cP), but 0.09 wt% GNP+PLLRC is lower (8.18 cP), already below the base fluid.
- At 50 °C, PLLRC viscosity is 5.34 cP, while GNP nanofluids range from 6.67 to 10.45 cP for 0.01–0.07 wt% GNP, and 4.26 cP for 0.09 wt% GNP, showing that the highest concentration gives both enhanced thermal conductivity and lower viscosity than the base fluid.
- At 70 °C, PLLRC is 3.16 cP, whereas 0.01–0.07 wt% nanofluids range from 3.89 to 7.07 cP; the 0.09 wt% nanofluid has the lowest viscosity (2.34 cP), about 26% lower than the base fluid, indicating reduced pumping resistance at high temperature.
- The fresh graphene nanofluid (0.09 GNP+PLLRC) achieves a 6.8% temperature drop at 30 °C, compared to 2.6% for the base fluid and 1.6% for the contaminated nanofluid, indicating a 4.2–5.2 %age point improvement in cooling efficiency at this temperature.
- At 40 °C, the reused nanofluid gives a temperature drop of 10.4%, slightly above the fresh nanofluid (9.7%) and significantly higher than the base fluid (7.9%), showing a 1.5–2.5 %age point improvement.
- Around 50 °C, the fresh nanofluid provides a 20% temperature reduction, compared to 10% for the base fluid and 12% for the contaminated nanofluid, demonstrating nearly a 10-percentage point enhancement.
- At higher temperatures (60–70 °C), the fresh nanofluid maintains a small but consistent advantage of 0.5–2.5 %age points over the base fluid in cooling performance.

Therefore, while nanofluids have clear lab benefits, maintaining clean coolant systems is crucial for optimal real-world performance. A minor limitation of this study is the lack of long-term cyclic testing to evaluate possible chemical or oxidative degradation of graphene in the coolant. While short-term results are promising, further research is needed to assess the long-term durability and stability of graphene nanofluids in real engine conditions. In summary, this study confirms graphene nanofluids as effective alternatives to traditional automotive coolants and highlights key challenges for their adoption. It lays the groundwork for future advances in more efficient, stable, and contamination-resistant cooling solutions in automotive thermal management.

CRediT authorship contribution statement

Wan Sharuzi Wan Harun: Writing – review & editing, Writing – original draft, Methodology, Formal analysis. **Maryam Sadat Kiai:** Writing – review & editing, Writing – original draft, Methodology, Formal analysis. **Chee Kuang Kok:** Writing – review & editing, Writing – original draft, Methodology, Formal analysis. **Lingenthiran Samylingam:** Writing – review & editing, Writing – original draft, Methodology, Formal analysis. **Navid Aslfattahi:** Writing – review & editing, Writing – original draft, Formal analysis. **Stephen Raj Jhonson:** Writing – review & editing, Writing – original draft, Methodology, Formal analysis. **Kumaran Kadirgama:** Writing – review & editing, Writing – original draft, Methodology, Formal analysis. **Clint K S:** Writing – review & editing, Writing – original draft, Methodology, Investigation, Formal analysis, Conceptualization. **A.S. Veerendra:** Writing – review & editing, Writing – original draft, Methodology, Formal analysis. **Sivaraos Subramonian:** Writing – review & editing, Writing – original draft, Methodology, Formal analysis.

Declaration of Competing Interest

The authors declare that they have no known competing financial interests or personal relationships that could have appeared to influence the work reported in this paper.

Acknowledgement

The authors acknowledge the financial support from the Ministry of Higher Education Malaysia through Fundamental Research Grant

Scheme (FRGS) FRGS/1/2024/TK09/UMP/01/1, and Universiti Malaysia PahangAl-Sultan Abdullah (UMPSA) under reference Grant RDU240110.

Appendix A. Supporting information

Supplementary data associated with this article can be found in the online version at doi:10.1016/j.nanoso.2026.101672.

Data availability

Data will be made available on request.

REFERENCES

[1] S. Jones-Jackson, R. Rodriguez, Y. Yang, L. Lopera, A. Emadi, Overview of current thermal management of automotive power electronics for traction purposes and future directions, IEEE Trans. Transp. Electrification 8 (2) (2022) 2412–2428.
[2] H. Liu, M. Wen, H. Yang, Z. Yue, M. Yao, A review of thermal management system and control strategy for automotive engines, J. Energy Eng. 147 (2) (2021) 03121001.
[3] H. Basir, S.A. Hosseini, S. Nasrollahnezhad, A. Jahangiri, M.A. Rosen, Investigation of engine's thermal management based on the characteristics of a map-controlled thermostat, Int. Commun. Heat. Mass Transf. 135 (2022) 106156.
[4] Marković J., Glavaš H., Barić T., Desnica E., editors. The Role Of Coolant In The Energy Balance Of Internal Combustion Engines. Proceedings of the XIV International Conference-Industrial Engineering and Environmental Protection (IIZS 2024); 2024: Zrenjanin: Technical Faculty "Mihajlo Pupin", Zrenjanin, University of Novi Sad.
[5] K. Kadirgama, L. Samylingam, N. Aslfattahi, M. Samykano, D. Ramasamy, R. Saidur, editors. Experimental investigation on the optical and stability of aqueous ethylene glycol/mxene as a promising nanofluid for solar energy harvesting. IOP conference series: materials science and engineering, IOP Publishing, 2021.
[6] M.H. Bargal, A.N. Allam, A.M. Zaki, M.E. Zayed, L.M. Alhems, H.M. Ali, Thermohydraulic performance augmentation and heat transfer enhancement of automotive radiators using nano-coolants: a critical review, J. Therm. Anal. Calorim. (2025) 1–53.
[7] L. Samylingam, N. Aslfattahi, C.K. Kok, K. Kadirgama, N. Sazali, M. Schmirler, et al., Green engineering with nanofluids: elevating energy efficiency and sustainability, J. Adv. Res. Micro Nano Eng. 16 (1) (2024) 19–34.
[8] L. Ben Said, L. Kolsi, K. Ghachem, M. Almeshaal, C. Maatki, Advancement of nanofluids in automotive applications during the last few years—a comprehensive review, J. Therm. Anal. Calorim. 147 (14) (2022) 7603–7630.
[9] M.A. Rahman, S.M. Hasnain, S. Pandey, A. Tapalova, N. Akylbekov, R. Zairov, Review on nanofluids: preparation, properties, stability, and thermal performance augmentation in heat transfer applications, ACS Omega 9 (30) (2024) 32328–32349.
[10] R.M. Mostafizur, M.G. Rasul, M.N. Nabi, R. Haque, M.I. Jahirul, Thermodynamic analysis of a flat plate solar collector with different hybrid nanofluids as working medium—a thermal modelling approach, Nanomaterials 13 (8) (2023) 1320.
[11] Y. Sawant, K. Pathare, R. Patel, P. Choughule, Nanofluids with recent application & future trends, Int. J. Innov. Eng. Res. Technol. 8 (06) (2021) 458–468.
[12] A.R. Urade, I. Lahiri, K. Suresh, Graphene properties, synthesis and applications: a review, Jom 75 (3) (2023) 614–630.
[13] T. Yusaf, A.S.F. Mahamude, K. Farhana, W.S.W. Harun, K. Kadirgama, D. Ramasamy, et al., A comprehensive review on graphene nanoparticles: preparation, properties, and applications, Sustainability 14 (19) (2022) 12336.
[14] G. Kadirgama, D. Ramasamy, K. Kadirgama, L. Samylingam, N. Aslfattahi, M. R. Chalak Qazani, et al., Characterization and machine learning analysis of hybrid alumina-copper oxide nanoparticles in therminol 55 for medium temperature heat transfer fluid, Sci. Rep. 15 (1) (2025) 8383.
[15] P. Falizi, S. Parhoodeh, A. Afsari, Comparing the effects of undoped and cobalt doped copper oxide nanoparticles on the enhancement of water thermal conductivity coefficient, Mater. Sci. Eng. B 297 (2023) 116713.
[16] W.-J. Ren, S. Lu, C.-Q. Yu, J. He, J. Chen, Carbon honeycomb structure with high axial thermal transport and strong robustness, Rare Met. 42 (8) (2023) 2679–2687.
[17] M. Aziz, D. Ramasamy, R. Kumaresan, S. Subramaniam, Investigation of heat transfer rate in automotive radiator with graphene nanofluid with simulation, Nexus Sustain. Energy Technol. J. 1 (1) (2025) 26–39.
[18] V. Kumar, S.R. Dadam, D. Zhu, J. Mehring, Fuel-economy performance analysis with exhaust heat recovery system on gasoline engine, SAE Int. J. Engines 15 (6) (2022) 825–848.
[19] M.M. Tawfik, Experimental studies of nanofluid thermal conductivity enhancement and applications: A review, Renew. Sustain. Energy Rev. 75 (2017) 1239–1253.
[20] Q. Khong Vu, D. Vu Minh, T. Nguyen Duy, T. Pham Minh, L. Nguyen The, A study of exhaust waste heat recovery in internal combustion engines, IOP Conference Series Materials Science Engineering 507 (1) (2019) 012028.
[21] L. Samylingam, N. Aslfattahi, C.K. Kok, K. Kadirgama, N. Sazali, K.W. Liew, et al., Enhancing lubrication efficiency and wear resistance in mechanical systems through the application of nanofluids: a comprehensive review, J. Adv. Res. Micro Nano Eng. 16 (1) (2024) 1–18.
[22] M. Fathi, M.M. Heyhat, M.Z. Targhi, S. Bigham, Porous-fin microchannel heat sinks for future micro-electronics cooling, Int. J. Heat. Mass Transf. 202 (2023) 123662.
[23] I. Samylingam, K. Kadirgama, N. Aslfattahi, L. Samylingam, D. Ramasamy, W. Harun, et al., editors. Review on thermal energy storage and eutectic nitrate salt melting point. IOP Conference Series: Materials Science and Engineering, IOP Publishing, 2021.
[24] H. Guo, X. Zhou, Z. Liu, Advanced lightweight structural materials for automobiles: Properties, manipulation, and perspective, Sci. Adv. Mater. 16 (5) (2024) 563–580.
[25] A. Candela, G. Sandrini, M. Gadola, D. Chindamo, P. Magri, Lightweighting in the automotive industry as a measure for energy efficiency: review of the main materials and methods, Heliyon 10 (8) (2024).
[26] C.A. Romero, P. Correa, E.A. Ariza Echeverri, D. Vergara, Strategies for reducing automobile fuel consumption, Appl. Sci. 14 (2) (2024) 910.
[27] B.R. Ponangi, V. Krishna, K.N. Seetharamu, Effect of Ultralow Concentrated Reduced Graphene Oxide Nanofluid on Radiator Performance, J. Heat. Transf. 143 (8) (2021).
[28] C. Selvam, T. Balaji, D.M. Lal, S. Harish, Convective heat transfer coefficient and pressure drop of water-ethylene glycol mixture with graphene nanoplatelets, Exp. Therm. Fluid Sci. 80 (2017) 67–76.
[29] F. Zakeri, M.R.S. Emami, Experimental and numerical investigation of heat transfer and flow of water-based graphene oxide nanofluid in a double pipe heat exchanger using different artificial neural network models, Int. Commun. Heat. Mass Transf. 148 (2023) 107002.
[30] C.T. Yaw, S.P. Koh, M. Sandhya, K. Kadirgama, S.K. Tiong, D. Ramasamy, et al., Heat transfer enhancement by hybrid nano additives—graphene nanoplatelets/cellulose nanocrystal for the automobile cooling system (Radiator), Nanomaterials 13 (5) (2023) 808.
[31] V. Kumar, S.K. Singh, V. Kumar, W. Jamshed, K.S. Nisar, Thermal and thermo-hydraulic behaviour of alumina-graphene hybrid nanofluid in minichannel heat sink: An experimental study, Int. J. Energy Res. 45 (15) (2021) 20700–20714.
[32] M. Sandhya, D. Ramasamy, K. Sudhakar, K. Kadirgama, W.S.W. Harun, Enhancement of the heat transfer in radiator with louvered fin by using Graphene-based hybrid nanofluids, IOP Conf. Series Mater. Sci. Eng. 1062 (1) (2021) 012014.
[33] Nogueira E. Thermal-hydraulic performance of Graphene Nanoribbon and Silicon Carbide nanoparticles in the multi-louvered radiator for cooling diesel engine. 2020.
[34] G. Dushyanthkumar, B. Praveenkumara, R. Shivashankar, D. Shrinivasa, N. Muthuraju, Experimental investigation of the enhancement of heat transfer rate in automobile radiator using low concentration hybrid nanofluids, J. Mines Met. Fuels 72 (11) (2024).
[35] X. Mei, X. Sha, D. Jing, L. Ma, Thermal conductivity and rheology of graphene oxide nanofluids and a modified predication model, Appl. Sci. 12 (7) (2022) 3567.
[36] P. Sonia, R. Chandrashekar, N. Hayder, K.S. Kumar Reddy, S. Lakhanpal, D. Arora, N.E.C. Prasad, Thermal analysis of radiator using sustainable graphene oxide nanofluid mixture of ethylene glycol and water, E3S Web Conf. 552 (2024) 01103.
[37] Y. Gao, Y. Xi, Y. Zhenzhong, A.P. Sasmito, A.S. Mujumdar, L. Wang, Experimental investigation of specific heat of aqueous graphene oxide Al2O3 hybrid nanofluid, Therm. Sci. 25 (1 Part B) (2021) 515–525.
[38] Sonia P., Chandrashekar R., Hayder N., Reddy K.S.K., Lakhanpal S., Arora D., Prasad N.C., editors. Thermal Analysis of Radiator Using Sustainable Graphene oxide Nanofluid Mixture of Ethylene Glycol and Water. E3S Web of Conferences; 2024: EDP Sciences.
[39] R.S. Mohammad, M.S. Aldlemy, A.M. Ahmed, M.W. Falah, S.J. Ahammed, Z. M. Yaseen, Thermal analysis of graphene-based nanofluids for energy system and economic feasibility, J. Nanomater. 2022 (1) (2022) 3530419.
[40] O. Khouri, H.R. Goshayeshi, S.B. Mousavi, S. Hosseini Nami, S. Zeinali Heris, Heat transfer enhancement in industrial heat exchangers using graphene oxide nanofluids, ACS Omega 9 (22) (2024) 24025–24038.
[41] S. Madderla, D. Ramasamy, K. Sudhakar, K. Kadirgama, W.S. Wan Harun, Heat transfer performance of a radiator with and without louvered strip by using Graphene-based nanofluids, J. Therm. Eng. 7 (6) (2021) 1315–1328.
[42] P. Kanti, K.V. Sharma, R.S. Khedkar, T.-u Rehman, Synthesis, characterization, stability, and thermal properties of graphene oxide based hybrid nanofluids for thermal applications: Experimental approach, Diam. Relat. Mater. 128 (2022) 109265.
[43] K. Tan, L. Samylingam, N. Aslfattahi, M.R. Johan, R. Saidur, Investigation of improved optical and conductivity properties of poly (methyl methacrylate)–MXenes (PMMA–MXenes) nanocomposite thin films for optoelectronic applications. O, pen Chem. 20 (1) (2022) 1416–1431.
[44] P.K. Kanti, M.P. Maiya, Rheology and thermal conductivity of graphene oxide and coal fly ash hybrid nanofluids for various particle mixture ratios for heat transfer applications: Experimental study, Int. Commun. Heat. Mass Transf. 138 (2022) 106408.
[45] C.R. Ratwani, K.S. Novoselov, A.M. Abdelkader, Applications and Mechanistic Insights Into Intrinsically Self-Healing Polymers With Multifunctional 2D Materials, SusMat (2025) e70028.
[46] C.T. Yaw, S.P. Koh, M. Sandhya, K. Kadirgama, S.K. Tiong, D. Ramasamy, et al., Heat Transfer Enhancement by Hybrid Nano Additives-Graphene Nanoplatelets/Cellulose Nanocrystal for the Automobile Cooling System (Radiator), Nanomater. (Basel) 13 (5) (2023).
[47] Kulandaivel S., Samykano M., Keng N.W., Suraparaju S.K., Rajamony R.K., editors. Assessing thermophysical properties of Nanostructured Cellulose Nano Crystal (CNC) and Graphene Nanoplatelets (GNP) Additives in Palm Oil-Based Heat Transfer Fluid. E3S Web of Conferences; 2024: EDP Sciences.
[48] P. Viprya, D. Kumar, S. Kowshik, Study of Different Properties of Graphene Oxide (GO) and Reduced Graphene Oxide (rGO), Eng. Proc. 59 (1) (2023) 84.

[49] A. Priyadarshini, M.K. Sutar, S. Pattnaik, Investigation of mechanical properties on functionally graded material reinforced with graphene nanoplatelets for biomedical applications, Compos. Interfaces 32 (2) (2025) 147–176.
[50] S.A. Hassanzadeh-Tabrizi, Precise calculation of crystallite size of nanomaterials: A review, J. Alloy. Compd. 968 (2023) 171914.
[51] M. Albozahid, H.Z. Naji, Z.K. Alobad, J.K. Wychowaniec, A. Saiani, Thermal, Mechanical, and Morphological Characterisations of Graphene Nanoplatelet/Graphene Oxide/High-Hard-Segment Polyurethane Nanocomposite: A Comparative Study, Polymers 14 (19) (2022).
[52] A. Moosa, M. Abed, Graphene preparation and graphite exfoliation, Turk. J. Chem. 45 (3) (2021) 493–519.
[53] M. Fang, H. Gu, B. Song, Z. Guo, S. Liu, Thickness and layer stacking order effects on complex optical conductivity and exciton strength of few-layer graphene: Implications for optical modulators and photodetectors, ACS Appl. Nano Mater. 5 (2) (2022) 1864–1872.
[54] I.A. Laghari, M. Samykano, A. Pandey, K. Kadirgama, Y.N. Mishra, Binary composite (TiO2-Gr) based nano-enhanced organic phase change material: Effect on thermophysical properties, J. Energy Storage 51 (2022) 104526.
[55] M. Pavía, K. Alajami, P. Estellé, A. Desforges, B. Vigolo, A critical review on thermal conductivity enhancement of graphene-based nanofluids, Adv. Colloid Interface Sci. 294 (2021) 102452.
[56] H. Lin, Q. Jian, X. Bai, D. Li, Z. Huang, W. Huang, et al., Recent advances in thermal conductivity and thermal applications of graphene and its derivatives nanofluids, Appl. Therm. Eng. 218 (2023) 119176.
[57] W. Jin, L. Jiang, L. Han, H. Huang, J. Zhang, M. Guo, et al., Investigation of thermal conductivity enhancement of water-based graphene and graphene/MXene nanofluids, J. Mol. Liq. 367 (2022) 120455.
[58] P. Kumar K, K. Deepthi Jayan, P. Sharma, M. Alruqi, Thermo-electro-rheological properties of graphene oxide and MXene hybrid nanofluid for vanadium redox flow battery: Application of explainable ensemble machine learning with hyperparameter optimization, FlatChem 43 (2024) 100606.
[59] S.U. Ilyas, R. Shamsuddin, T.K. Xiang, P. Estellé, R. Pendyala, Rheological profile of graphene-based nanofluids in thermal oil with hybrid additives of carbon nanotubes and nanofibers, J. Mol. Liq. 376 (2023) 121443.
[60] K.H. Dehnou, G.S. Norouzi, M. Majidipour, A review: Studying the effect of graphene nanoparticles on mechanical, physical and thermal properties of polylactic acid polymer, RSC Adv. 13 (6) (2023) 3976–4006.
[61] T. Thirugnanasambandan, Influence of graphene nanoparticles on thermal properties of the natural fiber-based hybrid composites, Nat. Fiber-Reinf. Compos. Therm. Prop. Appl. (2022) 219–237.
[62] T. Sathish, Ü. Ağbulut, M. Ubaidullah, R. Saravanan, J. Giri, S.F. Shaikh, Waste to fuel: A detailed combustion, performance, and emission characteristics of a CI engine fuelled with sustainable fish waste management augmentation with alcohols and nanoparticles, Energy 299 (2024) 131412.
[63] A.O. Borode, N.A. Ahmed, P.A. Olubambi, Electrochemical corrosion behavior of copper in graphene-based thermal fluid with different surfactants, Heliyon 7 (1) (2021) e05949.
[64] R.M. Mostafizur, M.G. Rasul, M.N. Nabi, Effect of surfactant on stability, thermal conductivity, and viscosity of aluminium oxide–methanol nanofluids for heat transfer applications, Therm. Sci. Eng. Prog. 31 (2022) 101302.